# KINETIC MODEL OF RADIATIVE RECOMBINATION PROCESSES IN 2H-$MoS_2$ CRYSTALS

**D. Dumchenko**

*Institute of Applied Physics, Academy of Sciences of Moldova, 5 Academiei str., MD-2028, Chisinau, Republic of Moldova*

## Abstract

Steady-state photoluminescence (PL) measurements revealed 2H-$MoS_2$ crystals. Two distinct radiative regions in the near infrared are performed. The first region consisting of several sharp lines is produced by bound excitons related to the halogen transport agent intercalated within the van der Waals gap of the layered compound. The second region is a broad spectral band, originates from the radiative recombination between an intrinsic defect center and the valence band in the conditions of a strong electron-phonon coupling. The spectral and temperature behavior of the PL intensity are described in the framework of a two-channel kinetic recombination model in thermal equilibrium conditions.

## 1. Introduction

2H-$MoS_2$ crystallizes in the hexagonal structure (space group $P6_3/mmc - D_{6h}^4$) consisting of covalently bonded S-Mo-S layers linked by weak van der Waals forces [1,2]. The unit cell contains two layers; the sulfur atoms in one layer are directly above the molybdenum atom in the next. These compounds are indirect band gap semiconductors [3,4,5]. It was shown [6,7] that the strong photoluminescence observed in synthetic $MoS_2$ crystals is caused by recombination of excitons bound to the neutral centers formed by the intercalation of halogen molecules $Cl_2$ placed in well-defined sites of the van der Waals gap.

In this work the results of experimental investigations and modelling, for the temperatures range 2÷150K and the energy range 0.7÷1.4eV are presented.

## 2. Experimental Results

The studied synthetic 2H-$MoS_2$ single crystals were grown by means of chemical vapor transport method, using chlorine $Cl_2$ as a transport agent. Naturally grown samples were cut from large natural bulk molybdenite crystals and then cleaved to produce fresh clean surfaces. The steady-state photoluminescence (PL) measurements were performed with a variable-temperature optical cryostat, a one-meter grating monochromator coupled to a cooled Ge-detector, and standard lock-in detection techniques. The luminescence excitation was provided by an Ar-ion laser ($\lambda$=514 nm). All spectra were corrected for the wavelength-dependent response of the optical system.

For investigated materials two distinct spectral regions were identified (fig. 1).

The first one is an excitonic region, located in the vicinity of the indirect band gap, consisting of several sharp zero-phonon lines and their vibronic replica. These lines are caused by recombination of excitons bound to halogen molecules, intercalated during the growth process.

The second spectral region is the IR vibronic broad band, characteristic also of natural 2H-$MoS_2$ crystals without halogen impurities. This region is associated with an intrinsic defect of the host lattice, which acts as a shunt channel and contributes to the thermal quenching of the exciton emission at $T$>60K.

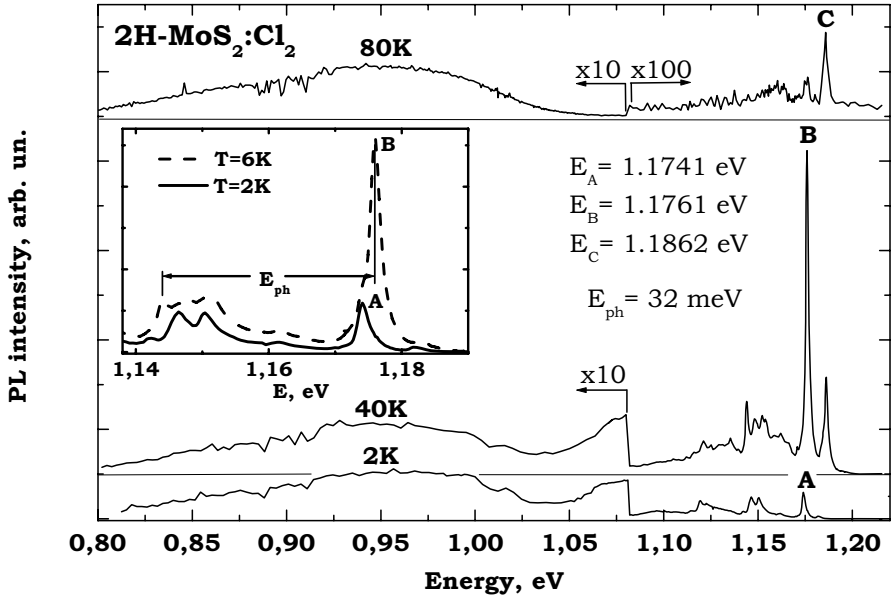


Fig. 1. Temperature evolution of the photoluminescence spectra of 2H-MoS2:Cl2 crystals.

In contrast to the broad band, the intensity of which remains constant up to almost 100K, the amplitudes of the sharp lines have a strong dependence on temperature. There were observed at least three zero-phonon spectral lines. The long wavelength line *A* is manifested only at lowest temperature (see insert to Fig.1).

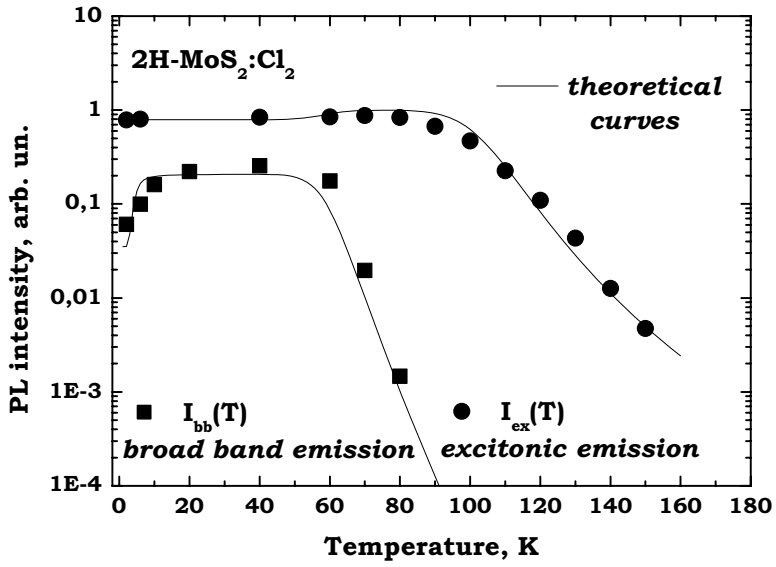


Fig. 2. Temperature dependence of the integrated intensity for the excitonic emission and the broadband emission.

The temperature increasing leads to the redistribution of the PL intensity to the sharp lines *B* and *C*. At *T*=6K the *A*-line can be observed just as a shoulder of the *B*-line. The *B*-line amplitude is the highest in the whole emission spectra up to *T*≈50K, when the *C*-line became dominating. At *T*>50K a fast thermal exponential quenching of the short wavelength emission occurs. The activation energy of this quenching is $E_{q1}$≈0.1eV. At *T*>80K already only the broad band luminescence is observed. The experimental temperature dependences of the broad band intensity as well as of the integral intensity of the three zero-phonon lines ($I_{ex}=I_A+I_B+I_C$) are presented in Fig.2 (dots).

## 3. Discussion

In order to describe the temperature behavior of the radiative spectral components we consider an *n*-type 2H-$MoS_2$ crystal structure that leads us to a level diagram (Fig. 3).

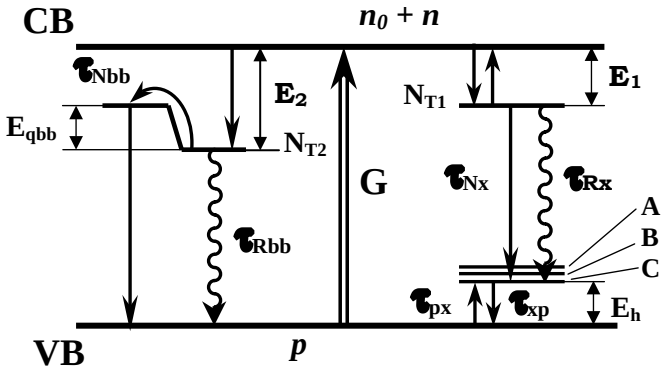


Fig. 3. Representation of level diagram with radiative and nonradiative processes.

Under the assumption of low-level excitation and thermal equilibrium the equations, which describe the kinetic behavior of minority carriers in n-type material, are given as follows:

$$\frac{dp}{dt} = G - p \cdot \upsilon_{th} \cdot \sigma_{px} \cdot \left(N_{T1}^{e} - N_{T1}^{x}\right) + \frac{N_{T1}^{x}}{\tau_{xp}} - p \cdot \frac{N_{T2}^{e}}{N_{T2}} \cdot \left(\frac{1}{\tau_{Rbb}} + \frac{1}{\tau_{Nbb}}\right),$$

$$\frac{dN_{T1}^{x}}{dt} = p \cdot \upsilon_{th} \cdot \sigma_{px} \cdot \left(N_{T1}^{e} - N_{T1}^{x}\right) - N_{T1}^{x} \cdot \left(\frac{1}{\tau_{Rx}} + \frac{1}{\tau_{Nx}} + \frac{1}{\tau_{xp}}\right).$$

Here *p* is the concentration of the minority holes, $N_{T1}^{e}$ and $N_{T2}^{e}$ the concentration of electron-occupied $T_1$-isoelectronic and $T_2$-deep centers, $N_{T1}^{x}$ the concentration of centers which have an exciton bound to the site, $\tau_{Rx}(\tau_{Nx})$ is the bound exciton radiative (nonradiative) recombination time, $\tau_{Rbb}(\tau_{Nbb})$ - $T_2$-levels radiative (nonradiative) time (hole shunt-path capture time), $\sigma_{px}$ is the hole capture cross section by electron occupied centers, $\upsilon_{th}$ is thermal velocity of minority carriers, $\tau_{xp}$ - isoelectronic trap exciton hole thermalization time and *G* is the excitation rate.

In *n*-type material the concentrations of electron-occupied isoelectronic and deep centers are in thermal equilibrium with the majority-carrier concentration

$$N_{T1}^{e} = f_{e1} \cdot N_{T2}, \quad N_{T2}^{e} = f_{e2} \cdot N_{T2} \ ,$$

where $f_{e1}$ and $f_{e2}$ are the electron occupancy probabilities of $T_1$ and $T_2$ centers respectively. In this case, from the steady-state solution

$$\frac{dN_{T1}^{x}}{dt} = 0 \ \text{ and } \ \frac{dp}{dt} = 0,$$

assuming that in considered temperature range all deep $T_2$ -centers ($E_{T2} \cong 0.3$ eV) are electron-occupied ($f_{e2} = 1, \ N_{T2}^{e} = N_{T2}$), and that at low-level excitation $p << N_{T2}$, $N_{T1}^{e} >> N_{T}^{x}$, the following relationship results for the quantum efficiencies of the excitonic radiative recombination $\eta_{Rx}(T)$ and the broad band emission $\eta_{Rbb}(T)$:

$$\eta_{Rx} = \frac{N_{T1}^{x}}{\tau_{Rx}} \cdot \frac{1}{G} = \left(1 + \frac{\tau_{Rx}}{\tau_{Nx}}\right)^{-1} \cdot \left[1 + \frac{\tau_{cp}}{\tau_{Rbb}} \cdot \left(1 + \frac{\tau_{Rbb}}{\tau_{Nbb}}\right) \cdot \left(1 + \frac{\tau_{Rx}}{\tau_{xp}}\right)\right]^{-1},$$

$$\eta_{Rbb} = \frac{p}{\tau_{Rbb}} \cdot \frac{1}{G} = \left(1 + \frac{\tau_{Rbb}}{\tau_{Nbb}}\right)^{-1} \cdot \left\{1 - \left[1 + \frac{\tau_{cp}}{\tau_{Rbb}} \cdot \left(1 + \frac{\tau_{Rbb}}{\tau_{Nbb}}\right) \cdot \left(1 + \frac{\tau_{Rx}}{\tau_{xp}}\right)\right]^{-1}\right\},$$

where $\tau_{cp} \equiv \left(\upsilon_{th} \cdot \sigma_{px} \cdot N_{T1}^{e}\right)^{-1}$, are defined as the capture time of holes by electron-occupied isoelectronic centers and by nonradiative shunt centers respectively.

The kinetic equations were solved numerically as function of temperature and density of traps $N_{T1}$ and $N_{T2}$. The curves obtained after calculations and the experimental points are presented in Fig. 2. How it can be seen, the curves obtained from our model fit with a good precision the temperature dependence of the quantum efficiencies of the excitonic emission and the broad band emission.

## References


[1] A. Wilson and A.D. Yoffe, Adv. Phys. 18, 193 (1969).

[2] W.J. Schutte, J.L. De Boer, and F. Jellinek, J. Solid State Chem 70, 207 (1987).

[3] A. Aruchamy (ed), *Photoelectrochemistry and Photovoltaics of Layered Semiconductors*, (Kluwer Academic Publishers, 1992).

[4] Th. Böker, R. Severin, A. Müller, C. Janowitz, R. Manzke, D. Vob, P. Krüger, A. Mazur, J. Pollmann, Phys. Rev. B 64, 235305 (2001).

[5] A. Klein, S. Tiefenbacher, V. Eyert, C. Pettenkofer, W. Jaegermann , Phys. Rev. B 64, 205416 (2001).

[6] L. Kulyuk, E. Bucher, L. Charron, E. Fortin, A. Nateprov, and O. Schenker, Nonlinear Opt. 29, 501 (2002).

[7] L. Kulyuk, L. Charron and E. Fortin, Phys. Rev. B 68, 075314 (2003).